

## Supplementary Information

### Monitoring thioredoxin redox with a genetically encoded red fluorescent biosensor

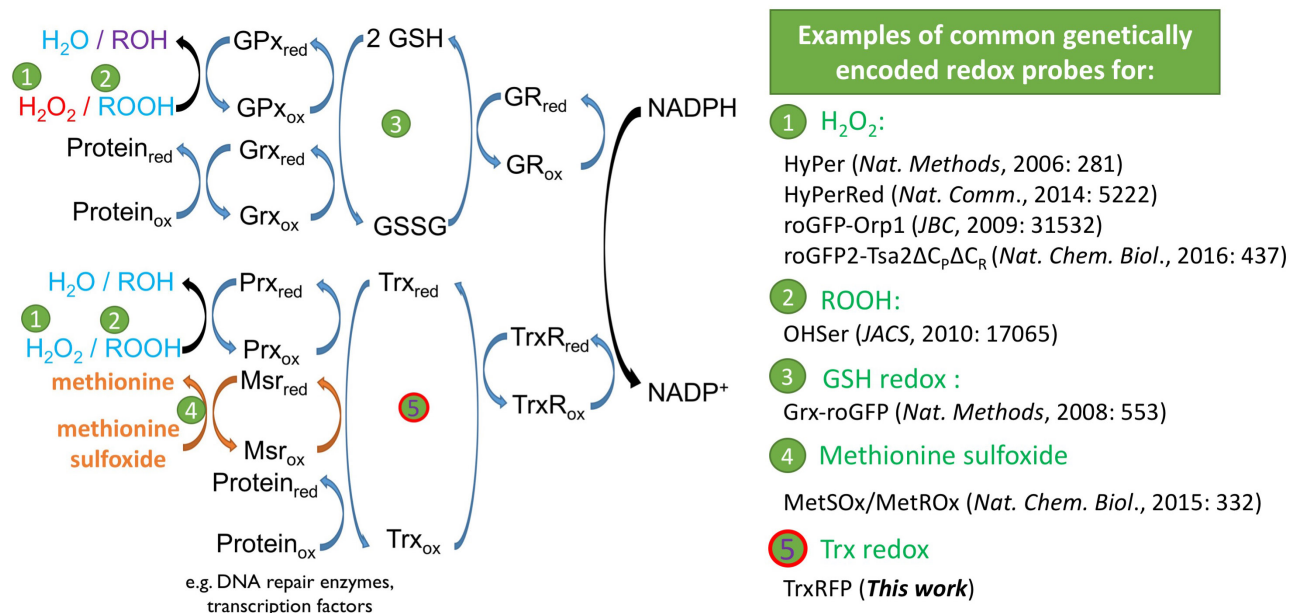
Yichong Fan<sup>1</sup>, Merna Makar<sup>2</sup>, Michael X. Wang<sup>2</sup>, and Hui-wang Ai<sup>1,2\*</sup>

<sup>1</sup>The Environmental Toxicology Graduate Program, and <sup>2</sup>Department of Chemistry, University of California Riverside, 501 Big Springs Road, Riverside, CA, 92521, USA

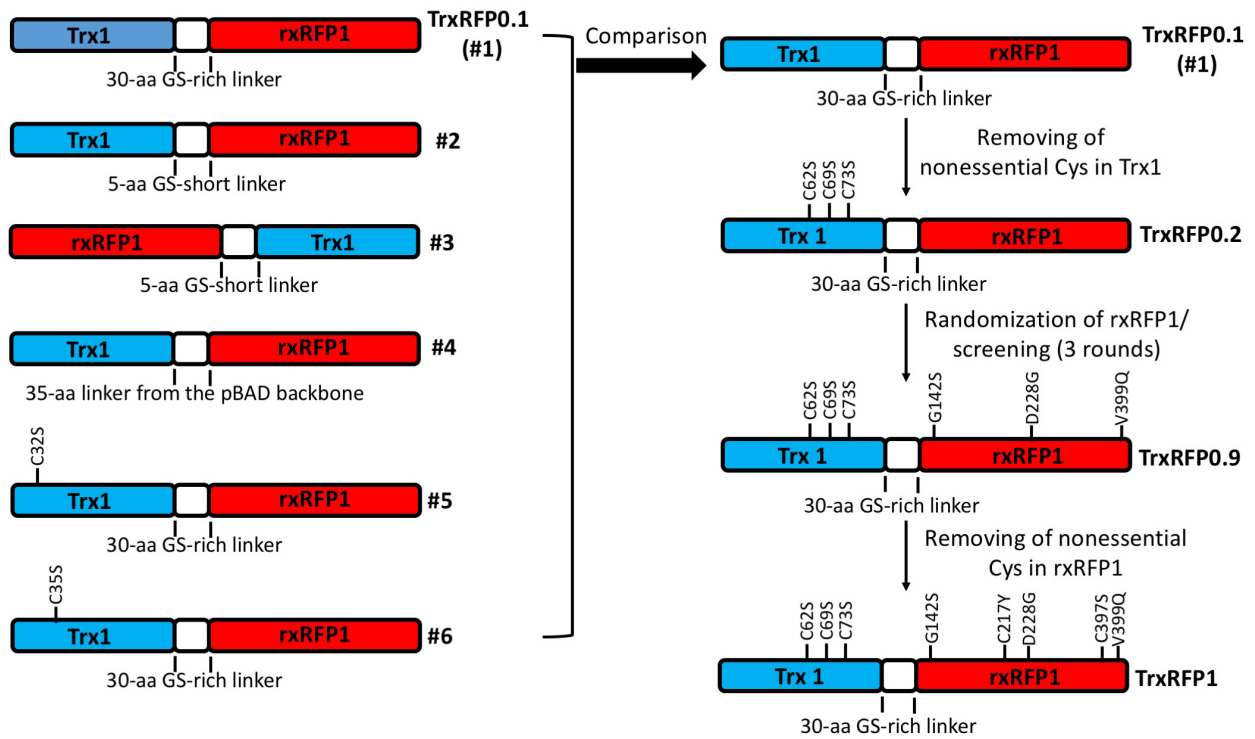
Correspondence should be sent to: [huiwang.ai@ucr.edu](mailto:huiwang.ai@ucr.edu)

## Supplementary Results

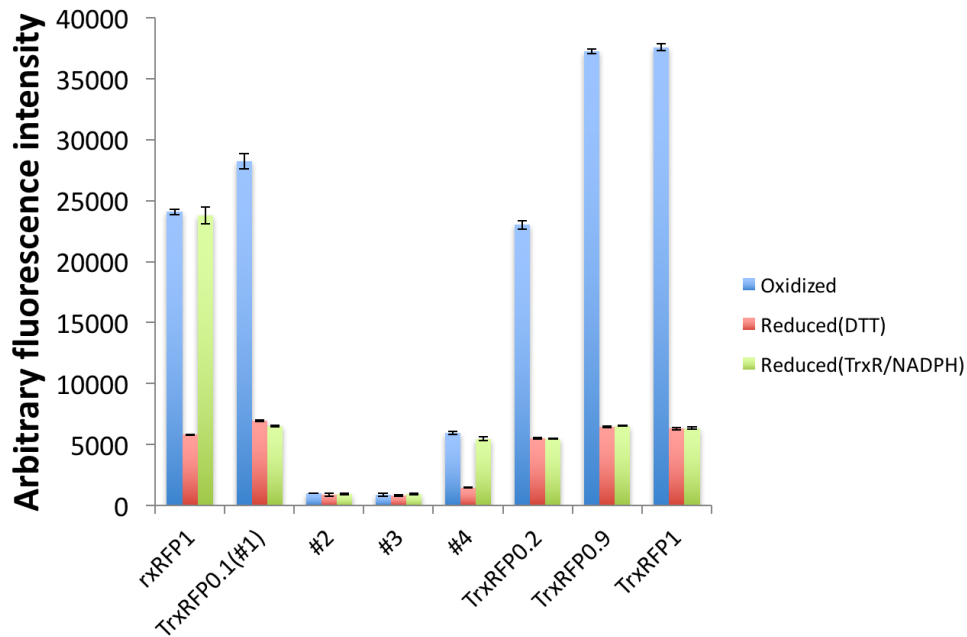
### Supplementary Figures



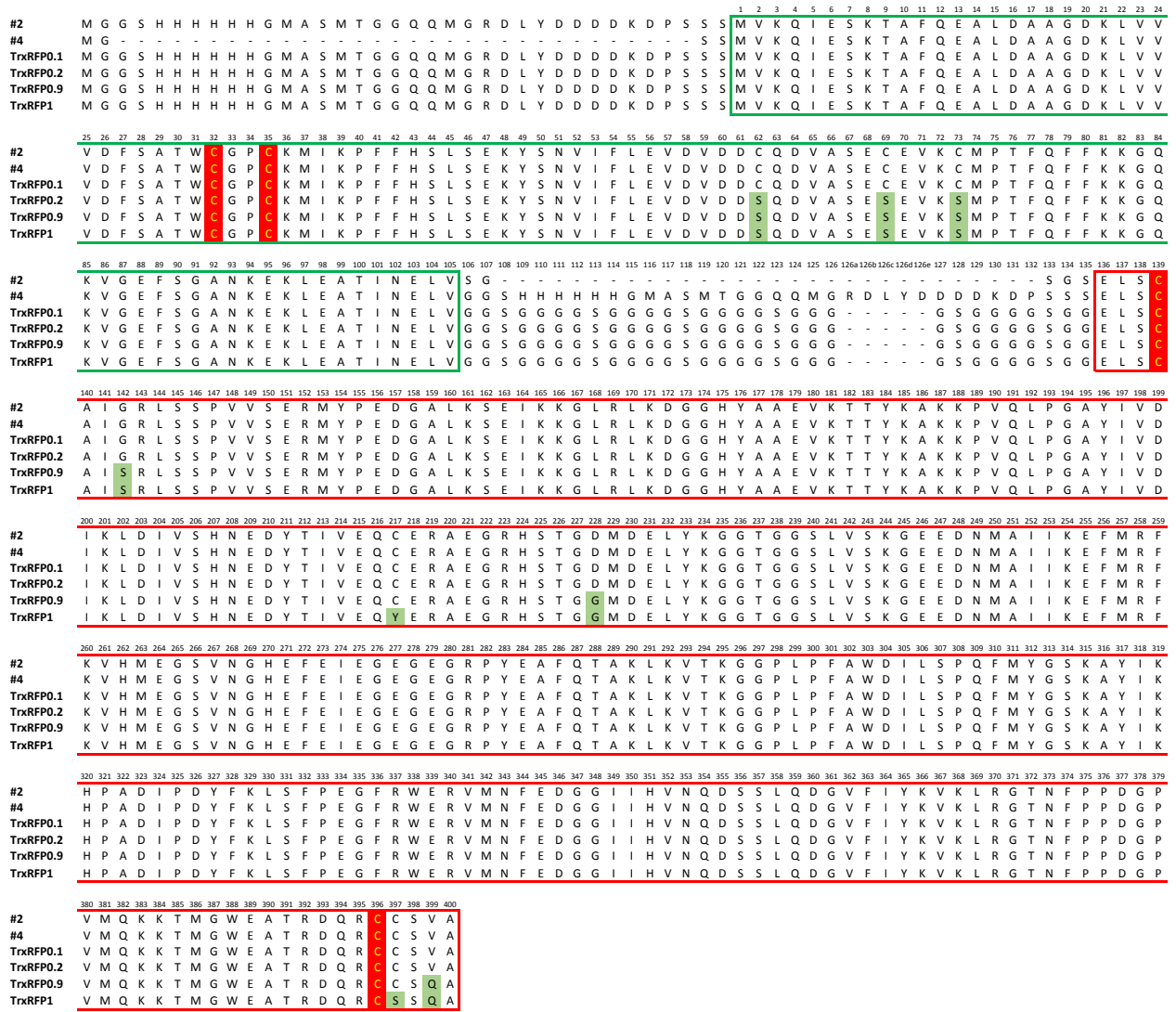
**Supplementary Figure 1.** Redox reactions of the glutathione and thioredoxin (Trx) redox systems. Both systems are coupled with the oxidation of NADPH and the reduction of reactive oxygen species (ROS). Also shown are examples of some existing genetically encoded redox probes. Prior to this work, no genetically encoded biosensor had been developed for probing the redox changes of Trx.



**Supplementary Figure 2.** The process to engineer TrxRFP1. Also shown are topological information, linker lengths, and critical mutations introduced to each variant.

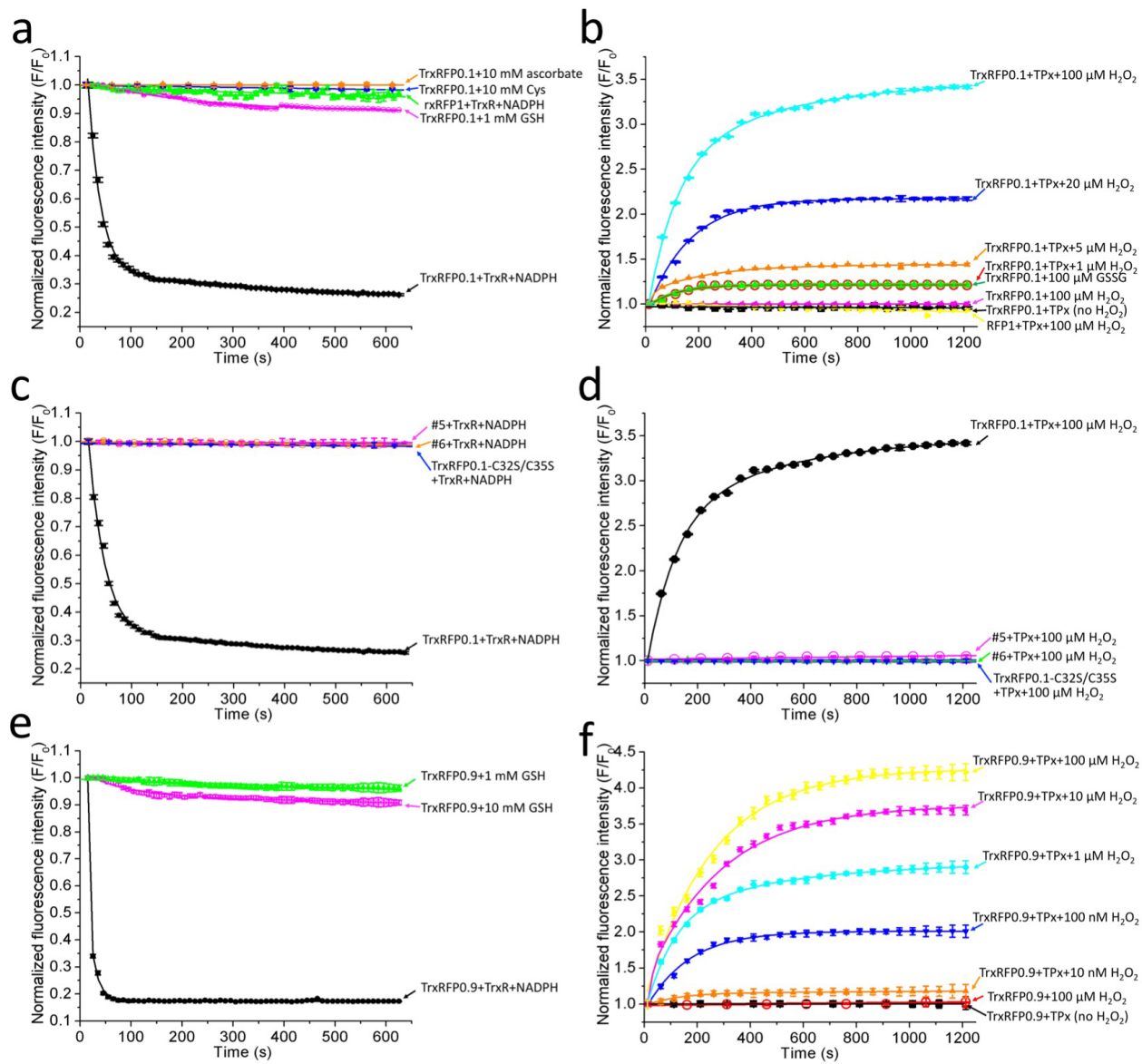


**Supplementary Figure 3.** Fluorescence of the indicated proteins at the same concentration (1  $\mu$ M) in their oxidized states and their reduced states maintained by DTT (10 mM) or recombinant human TrxR1 (10  $\mu$ M)/NADPH (200  $\mu$ M). Data are represented as mean and s.d. of three independent experiments.

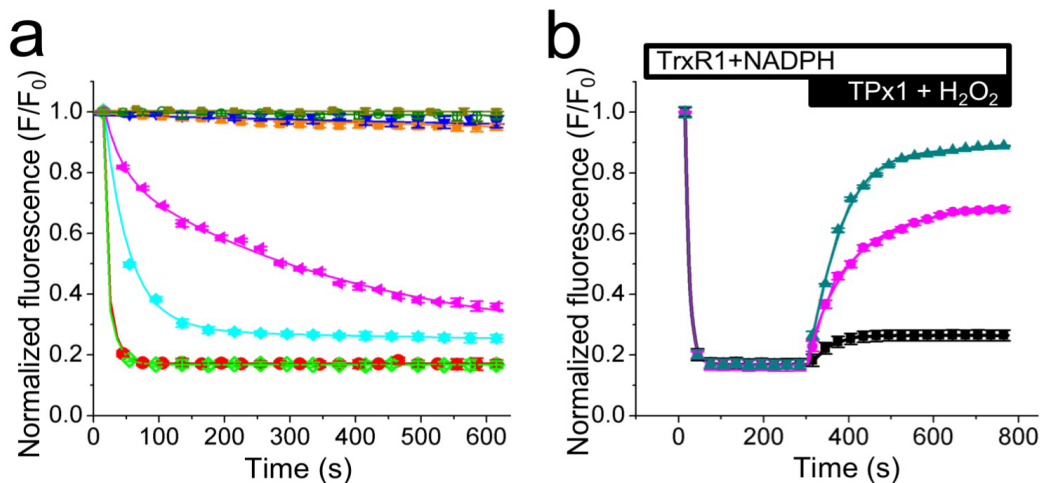


**Supplementary Figure 4.** Sequence alignment of TrxRFP1 and some earlier variants described in this work. The sequences derived from Trx1 and rxRFP1 are in a green and a red box, respectively. All four critical cysteines are highlighted with yellow fonts on red background. All mutations are highlighted with green shaded background.

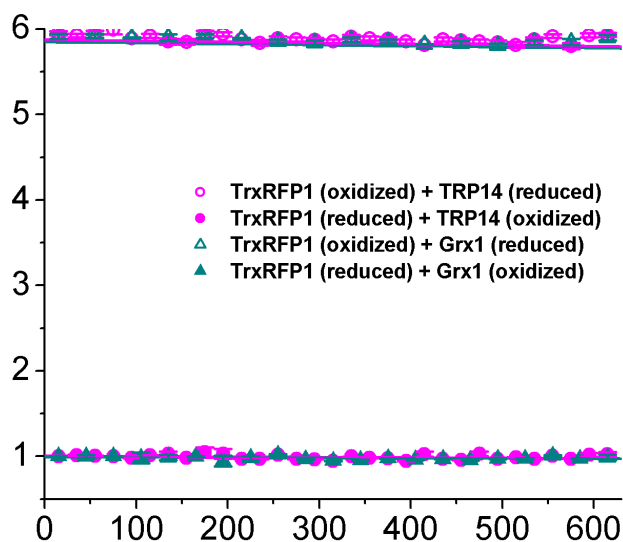




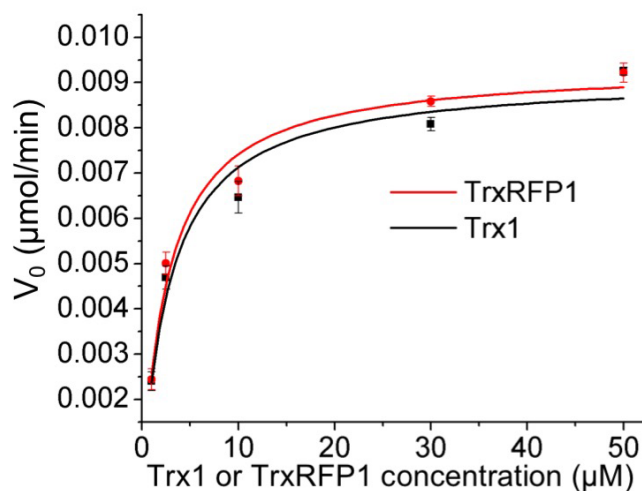
**Supplementary Figure 5.** Fluorescence responses of TrxRFP mutants to indicated reducing and oxidizing enzymes and compounds. Unless otherwise specified, 1  $\mu$ M each sensor protein, 10  $\mu$ M recombinant human TrxR1 and 200  $\mu$ M NADPH were used for enzymatic reduction reactions; 0.5  $\mu$ M each sensor protein and 0.5  $\mu$ M recombinant human TPx1 were used for enzymatic oxidation reactions. Data are represented as mean and s.d. of three independent experiments.



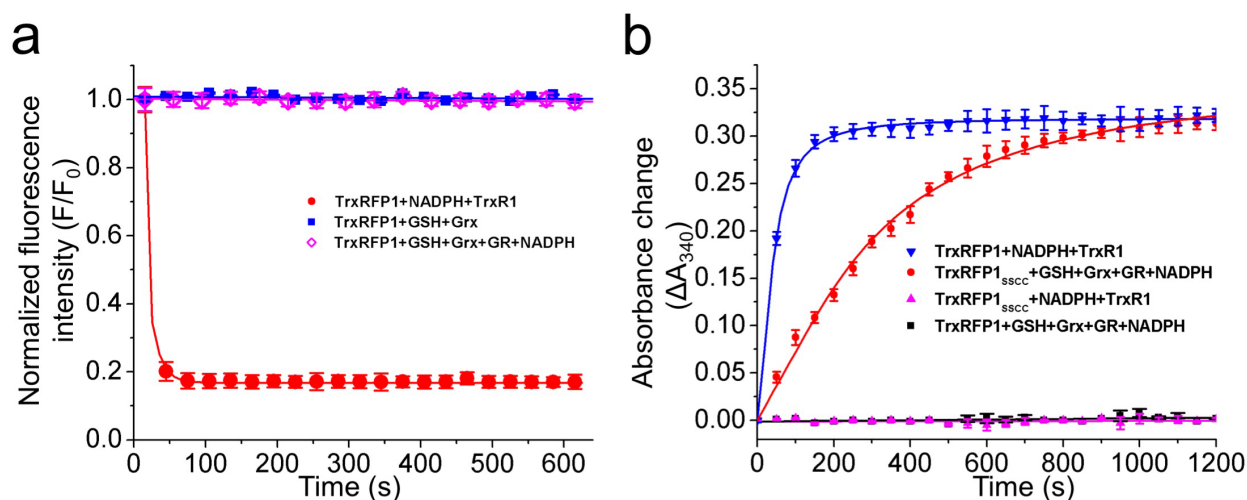
**Supplementary Figure 6.** (a) Kinetic traces for the reduction of oxidized proteins (from top to bottom: ■ TrxRFP1 + 10 mM L-ascorbic acid, ○ TrxRFP1 + 10 mM L-cysteine, ▼ TrxRFP1 + 10 μM TrxR1 + NADPH, ■ TrxRFP1 + 1 mM GSH, ▲ TrxRFP1 + 2 μM TrxR1 + NADPH, ◆ TrxRFP1 + 5 μM TrxR1 + NADPH, ● TrxRFP1 + 10 μM TrxR1 + NADPH, and ◇ TrxRFP1 + 10 μM TrxR1 + NADPH + 100 μM GSSG). (b) Kinetic traces for TrxRFP1 reduced with 10 μM recombinant human TrxR1 / 200 μM NADPH and reversibly oxidized by addition of TPx1/H<sub>2</sub>O<sub>2</sub> (■ 0.5 μM TPx1 + 10 μM H<sub>2</sub>O<sub>2</sub>, ● 0.5 μM TPx1 + 200 μM H<sub>2</sub>O<sub>2</sub>, and ▲ 2 μM TPx1 + 200 μM H<sub>2</sub>O<sub>2</sub>). TrxR1 used in these experiments was recombinant human TrxR1 with only partial activity (also see Fig. 1 and Online Methods). Data are represented as mean and s.d. of three independent experiments.



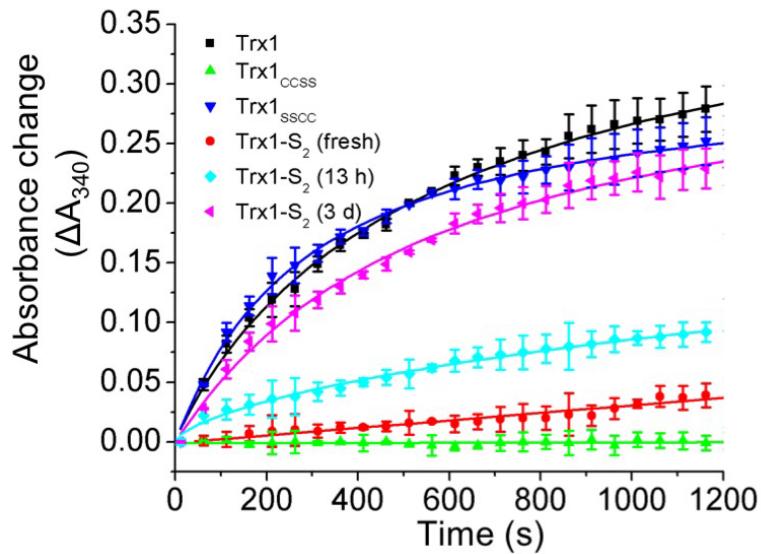
**Supplementary Figure 7.** Kinetic traces for the fluorescence of TrxRFP1 (1 μM) mixed with 5 μM each of Trx-like, redox-sensitive proteins such as glutaredoxin 1 (Grx1) and thioredoxin (Trx)-related protein TRP14, indicating that no reaction took place and TrxRFP1 is a specific biosensor. Data are represented as mean and s.d. of three independent experiments.



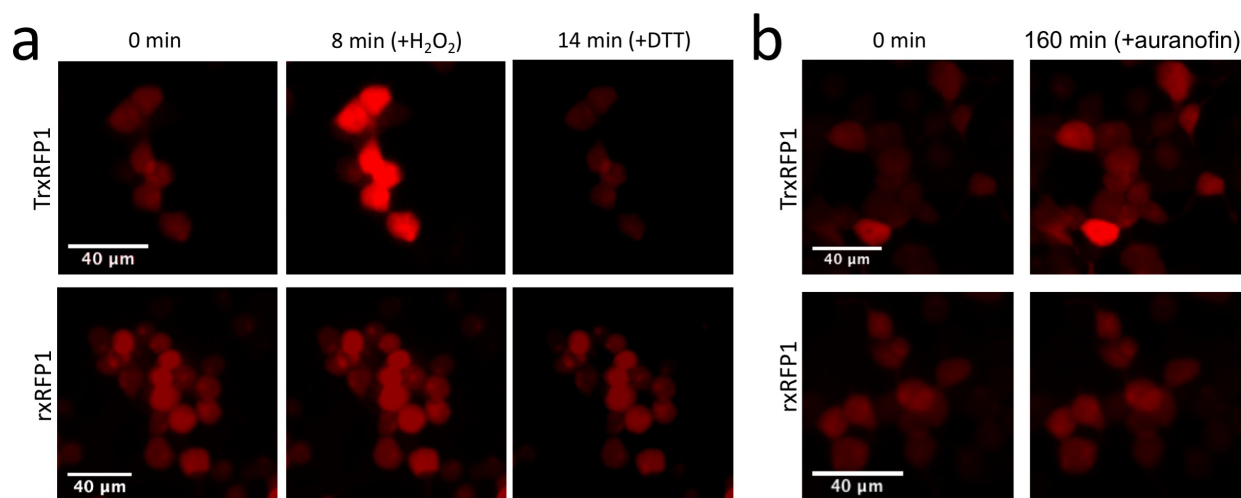
**Supplementary Figure 8.** A comparison of enzyme kinetics of TrxRFP1 and Trx1 for rat TrxR1. Assays were conducted at room temperature as 1-mL reaction mixtures consisting of 10 nM rat TrxR, 2 mM EDTA, 200  $\mu$ M NADPH, and 100 mM sodium phosphate (pH 7.4). NADPH oxidation was spectrophotometrically monitored at 340 nm.  $K_M$  values were obtained by fitting the data with the Michaelis-Menten equation ( $K_M = 2.63 \pm 0.49 \mu$ M or  $2.83 \pm 0.69 \mu$ M TrxRFP1 and Trx1, respectively). Data are represented as mean and s.d. of three independent experiments at each protein concentration.



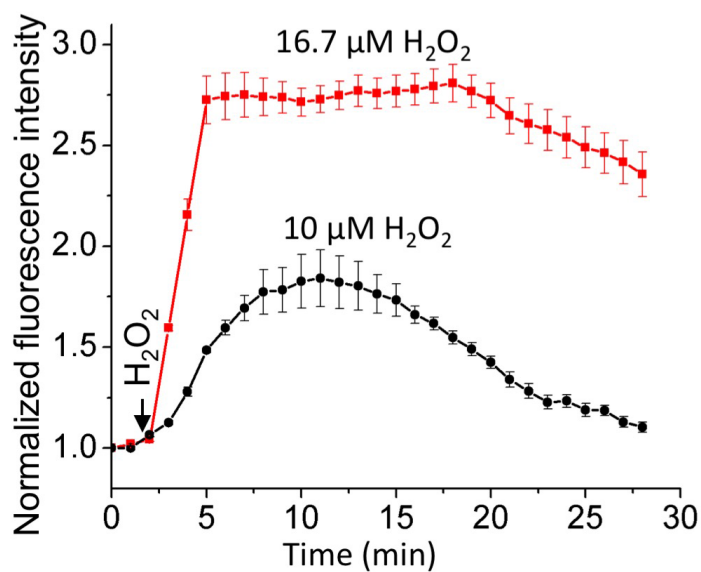
**Supplementary Figure 9.** (a) Kinetic traces for the fluorescence of TrxRFP1 (1  $\mu$ M) treated with 10  $\mu$ M recombinant TrxR1 and 200  $\mu$ M NADPH (red), or 10 mM glutathione and 5  $\mu$ M Grx1 (blue), or 10 mM glutathione, 5  $\mu$ M Grx1, 45 nM glutathione reductase, and 200  $\mu$ M NADPH (magenta). (b) Kinetic traces for the absorbance at 340 nm for the indicated reactions: 60  $\mu$ M TrxRFP1 (blue) or TrxRFP1<sub>sscc</sub> (C32S/C35S/S62C/S69C; magenta) treated with 10  $\mu$ M recombinant human TrxR1 and 200  $\mu$ M NADPH, or 60  $\mu$ M TrxRFP1 (black) or TrxRFP1<sub>sscc</sub> (red) treated with 10 mM glutathione, 5  $\mu$ M Grx1, 45 nM glutathione reductase, and 200  $\mu$ M NADPH. Data are represented as mean and s.d. of three independent experiments.



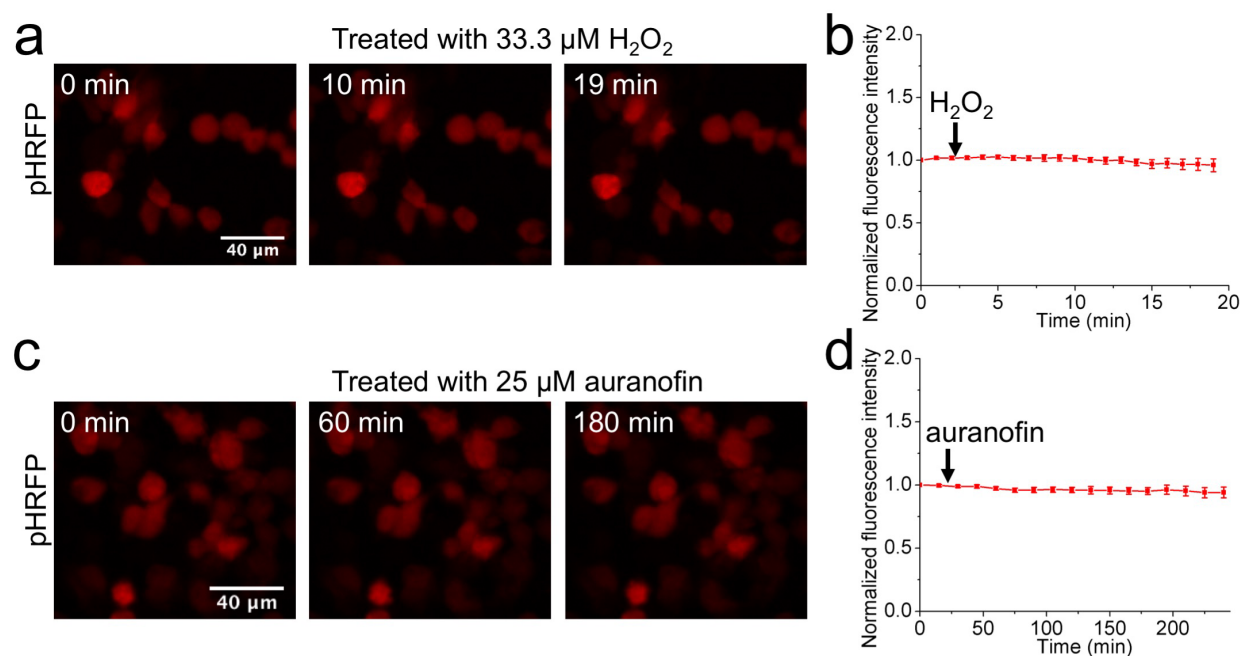
**Supplementary Figure 10.** A comparison of Trx1 and several Trx1 variants in response to glutaredoxin/glutathione reduction. Different Trx1 mutants (20  $\mu\text{M}$ ) were treated with a mixture containing NADPH (200  $\mu\text{M}$ ), glutathione reductase (60 nM), Grx1 (1  $\mu\text{M}$ ), and GSH (10 mM). The consumption of NADPH was monitored by absorbance at 340 nm. The wild-type Trx1, in which two intramolecular disulfide bonds could form in air, responded to the reduction. So did Trx1<sub>SSCC</sub> (32S/35S/62C/S69C), which could form one non-active-site disulfide bond. In contrast, Trx1<sub>CCSS</sub> (32C/35C/62S/S69S), which could form one active-site disulfide bond, showed no response. Trx1-S<sub>2</sub>, which is the wild-type Trx1 reduced by DTT and re-oxidized by a half amount of insulin, was prepared according to the procedure described in Reference 37. Trx1-S<sub>2</sub> is supposed to have an active-site disulfide and three non-active site free thiols. Freshly prepared Trx1-S<sub>2</sub> (red) only triggered a small response. We stored the prepared protein in a sealed tube at 4°C and observed increased responses after 13-hour (cyan) and 3-day (magenta) storage. Since it is difficult to exclude all oxygen in air, Trx1-S<sub>2</sub> was likely not completely pure at the beginning and slowly oxidized over time to form the non-active-site disulfide bond. Combining this with our results on Trx1<sub>SSCC</sub> and Trx1<sub>CCSS</sub>, we conclude that the glutaredoxin/glutathione system is involved in the reduction of the non-active-site disulfide bond, but not the active-site disulfide bond, of Trx1. Data are represented as mean and s.d. of three independent experiments.



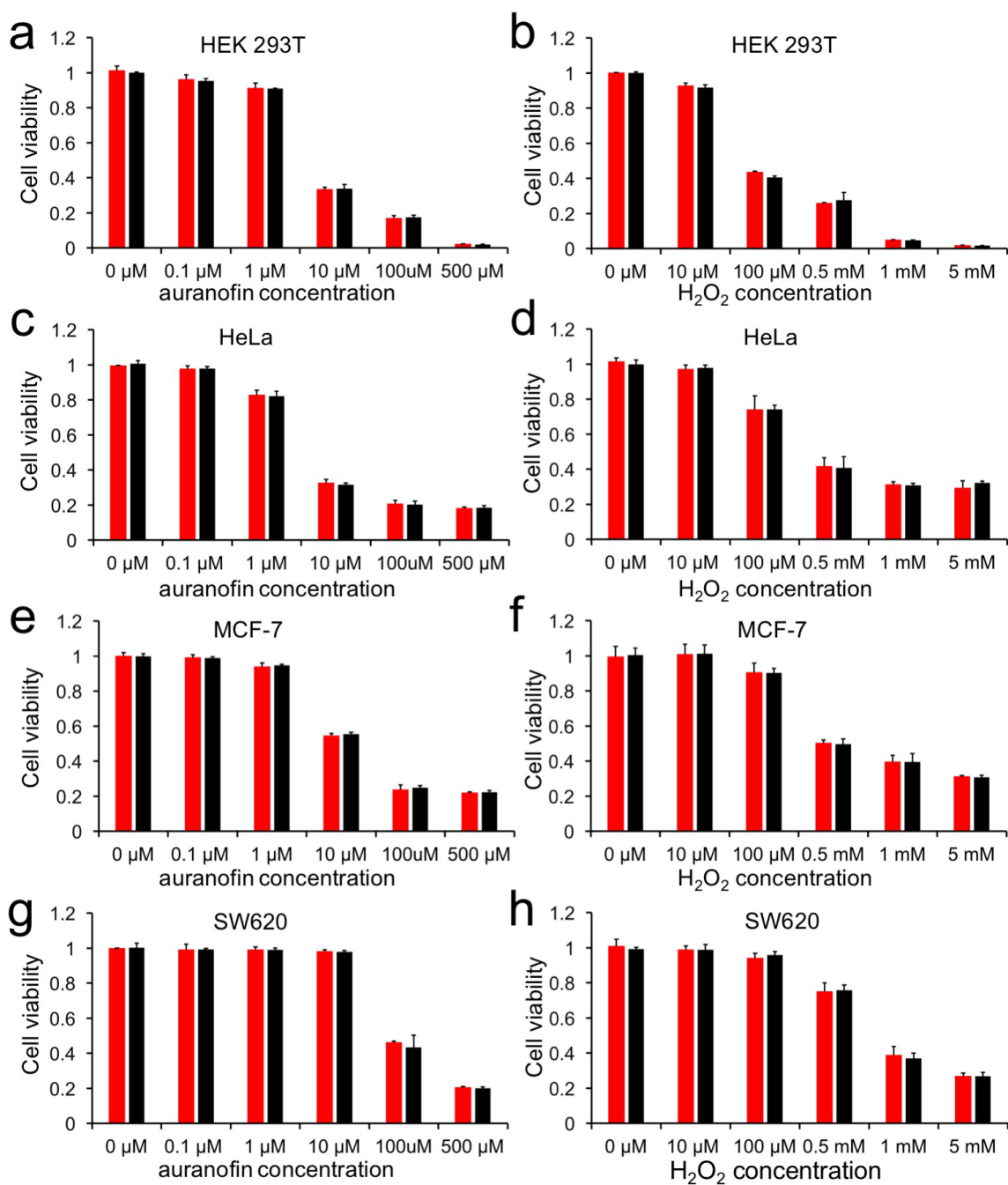
**Supplementary Figure 11.** Time-lapse fluorescence images of TrxRFP1 and rxRFP1 in HEK 293T cells, sequentially treated with 16.7  $\mu\text{M}$   $\text{H}_2\text{O}_2$  and 10 mM DTT (a), or treated with 10  $\mu\text{M}$  auranofin (b), showing  $\text{H}_2\text{O}_2$ - and auranofin- induced fluorescence changes for TrxRFP1 but not for rxRFP1 (Scale bar = 40  $\mu\text{m}$ ).



**Supplementary Figure 12.** Time-lapse responses of TrxRFP1 in HEK 293T cells to two different concentrations of  $\text{H}_2\text{O}_2$  in the imaging medium, showing that the process of Trx oxidation is reversible and Trx was reduced more quickly by intracellular systems when the lower  $\text{H}_2\text{O}_2$  concentration was used. The intensities were normalized to the value at  $t = 0$  min and shown as the mean and s.d. of randomly selected eight cells from three independent replicates. The arrows indicate the time points for addition of  $\text{H}_2\text{O}_2$ .

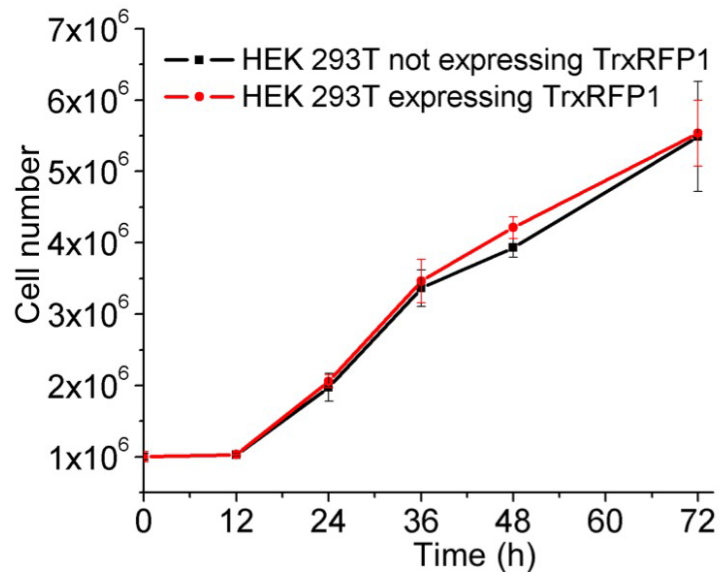


**Supplementary Figure 13.** Time-lapse responses of a genetically encoded pH indicator pHRFP in HEK 293T cells to 33.3  $\mu\text{M}$   $\text{H}_2\text{O}_2$  (**a,b**) or 25  $\mu\text{M}$  auranofin (**c,d**), showing no substantial pH change during these treatments (Scale bar = 40  $\mu\text{m}$ ). In panels **b** and **d**, the intensities were normalized to the value at  $t = 0$  min and shown as the mean and s.d. of randomly selected eight cells from three independent replicates. The arrows indicate the time points for addition of  $\text{H}_2\text{O}_2$  or auranofin.



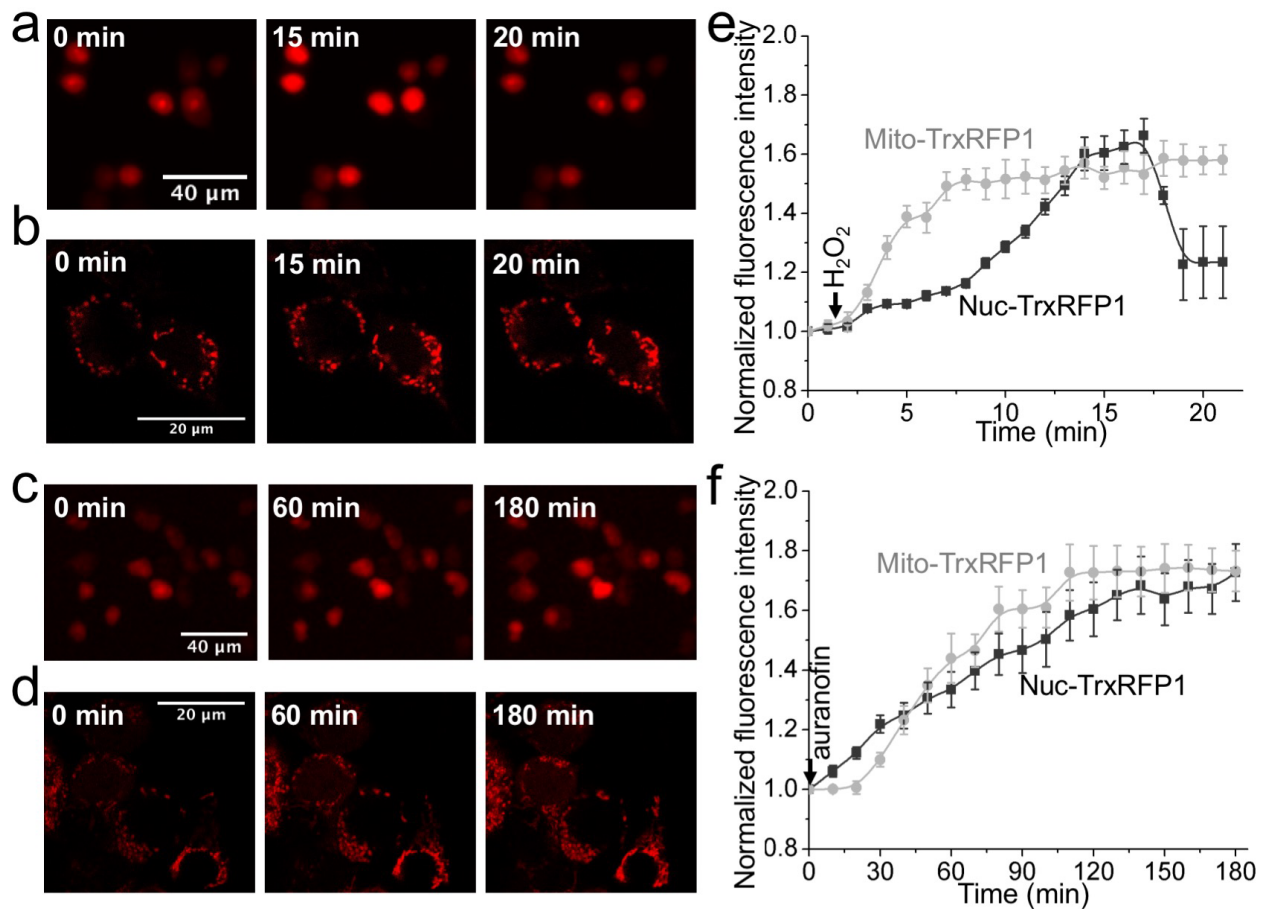
**Supplementary Figure 14.** The viability of various types of cells with (red) or without (black) overexpression of TrxRFP1 in response to auranofin or  $H_2O_2$ , indicating that expression of TrxRFP1 does not affect cellular redox homeostasis. Cells were treated with the indicated concentrations of auranofin or  $H_2O_2$  for 24 h, and cell viabilities were determined using a Promega RealTime-Glo MT cell viability assay. Data are shown as mean and s.d. of three independent experiments. The two-tailed Student's t-test was used to determine the significance of the differences at each concentration ( $p > 0.1$  for all comparisons).



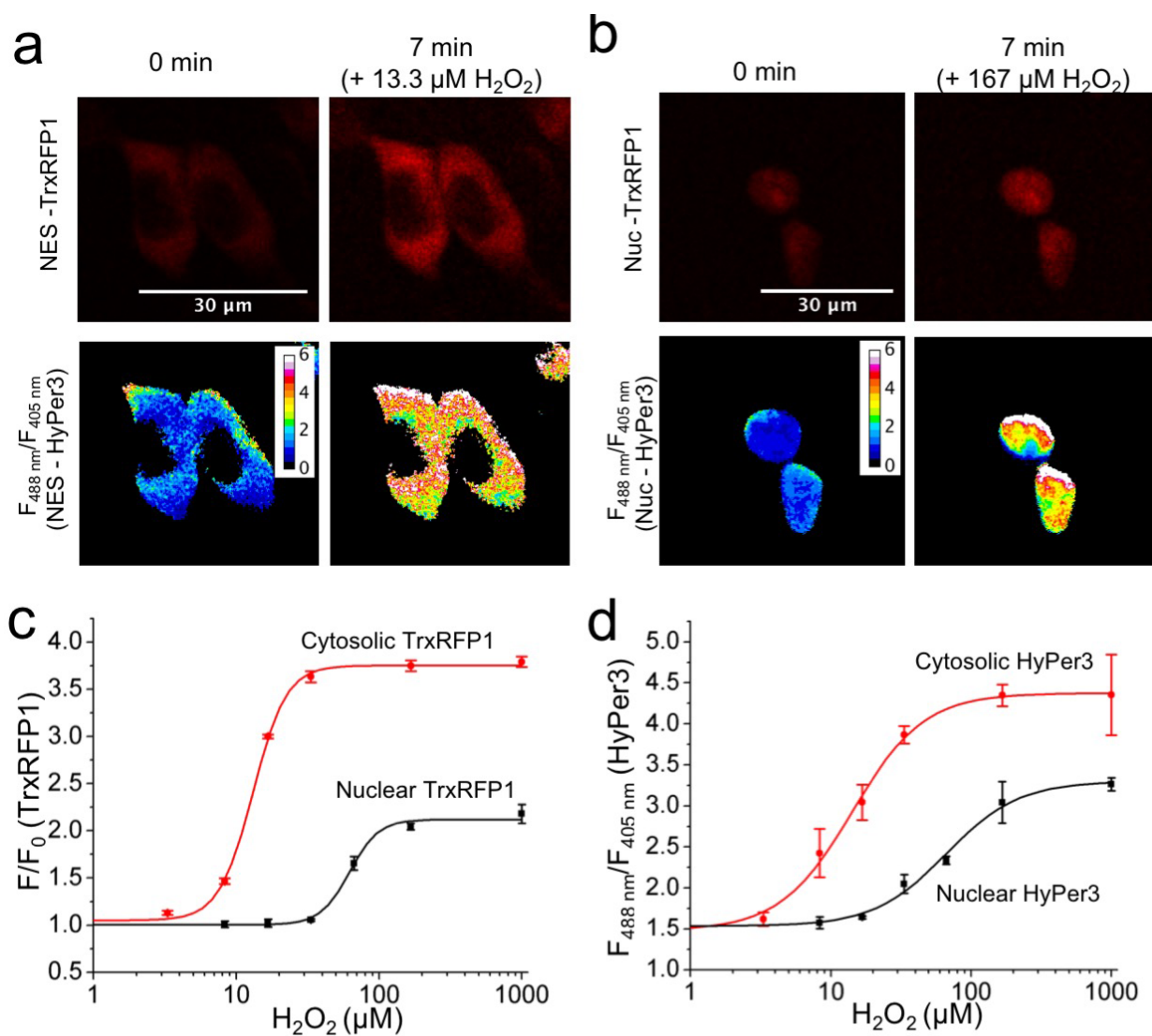


**Supplementary Figure 15.** A comparison of the growth of HEK 293T cells expressing or not expressing TrxRFP1. Data are shown as mean and s.d. of three independent experiments. An unpaired Student's t-test was used to determine the significance of the differences at each time point ( $p > 0.1$  for all comparisons).

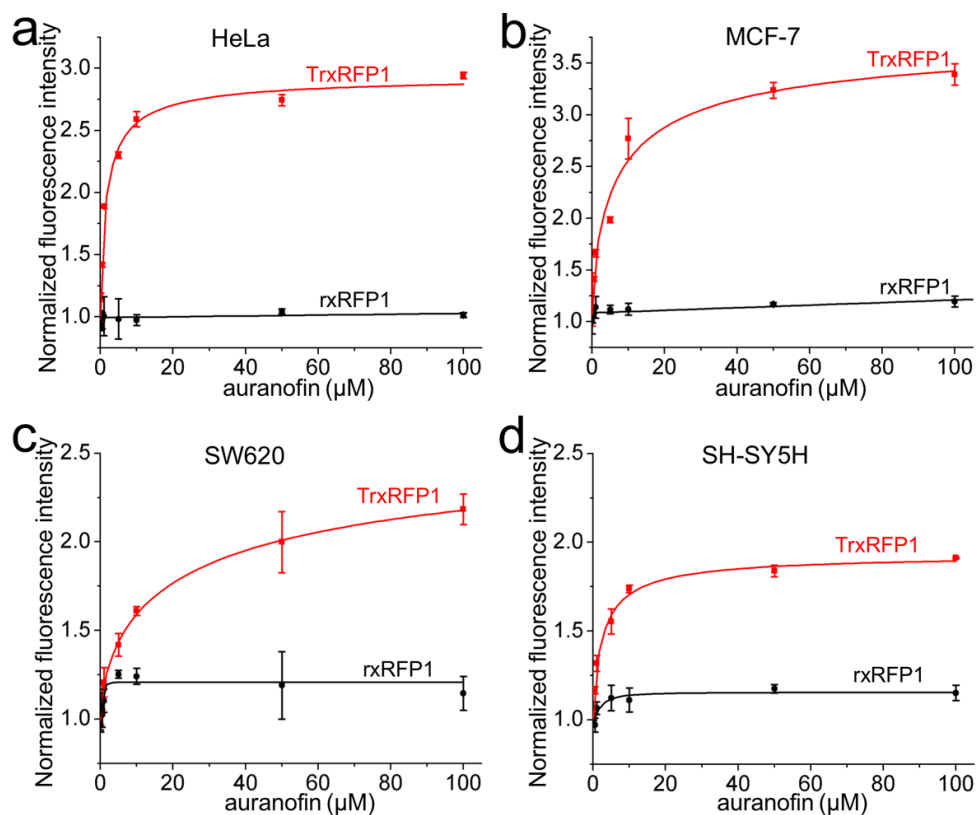




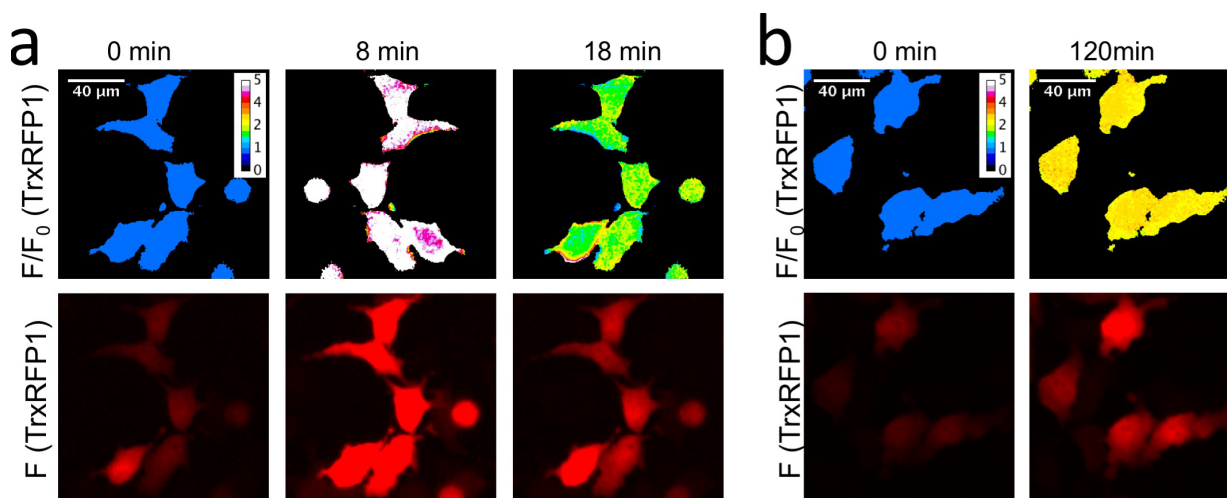
**Supplementary Figure 16.** Time-lapse responses of nuclear (**a,c**) and mitochondrial (**b,d**) TrxRFP1 in HEK 293T cells to H<sub>2</sub>O<sub>2</sub> (**a,b**) and auranofin (**c,d**). 66.7  $\mu\text{M}$  H<sub>2</sub>O<sub>2</sub> was used to treat cells at  $t = 1.1$  min in panels **a** and **b**. 10  $\mu\text{M}$  and 20  $\mu\text{M}$  auranofin were used to treat cells at  $t = 0$  min in panels **c** and **d**, respectively. In panels **e** and **f**, the intensities were normalized to the value at  $t = 0$  min and shown as the mean and s.d. of randomly selected eight cells from three independent replicates. The arrows indicate the time points for addition of H<sub>2</sub>O<sub>2</sub> or auranofin (Scale bar = 40  $\mu\text{m}$  for panels **a** and **c**; 20  $\mu\text{m}$  for panels **b** and **d**).



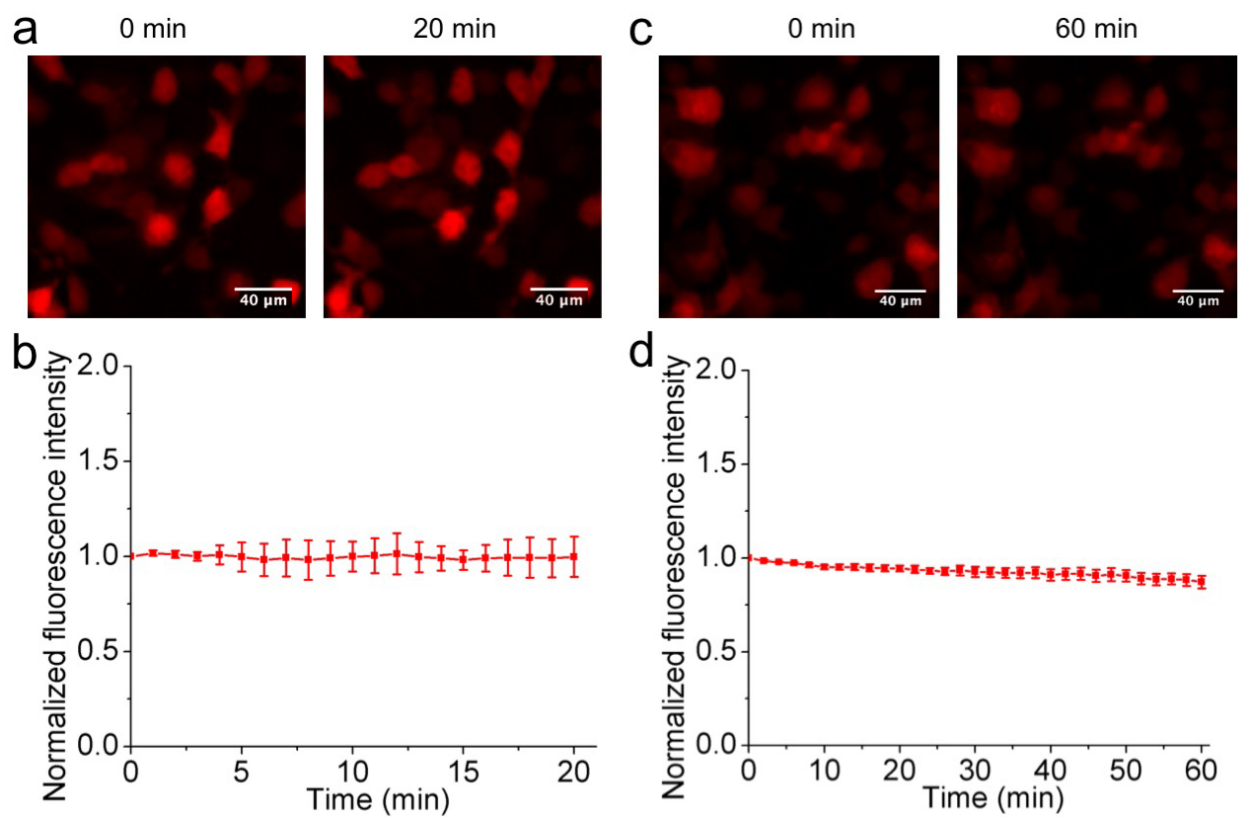
**Supplementary Figure 17.** (a,b) Time-lapse responses of cytosolic (a) and nuclear (b) TrxRFP1 and HyPer3 in HEK 293T cells to 13.3  $\mu\text{M}$  (a) or 167  $\mu\text{M}$  (b)  $\text{H}_2\text{O}_2$  (Scale bar = 30  $\mu\text{m}$ ). Cytosolic expression was enabled by using a nuclear export sequence (NES). A nuclear localization sequence (NLS) was used for nuclear targeting. HyPer3 is an excitation-ratiometric biosensor and the HyPer3 images are pseudocolored according to excitation ratios (488 nm excitation/405 nm excitation). Higher concentrations of  $\text{H}_2\text{O}_2$  were needed to trigger the responses of nuclear TrxRFP1 and HyPer3 than cytosolic TrxRFP1 and HyPer3. (c,d) Fluorescence responses of cytosolic and nuclear TrxRFP1 (c) or HyPer3 (d) in HEK 293T to various concentrations of  $\text{H}_2\text{O}_2$ . Data are shown as mean and s.d. of three independent experiments.



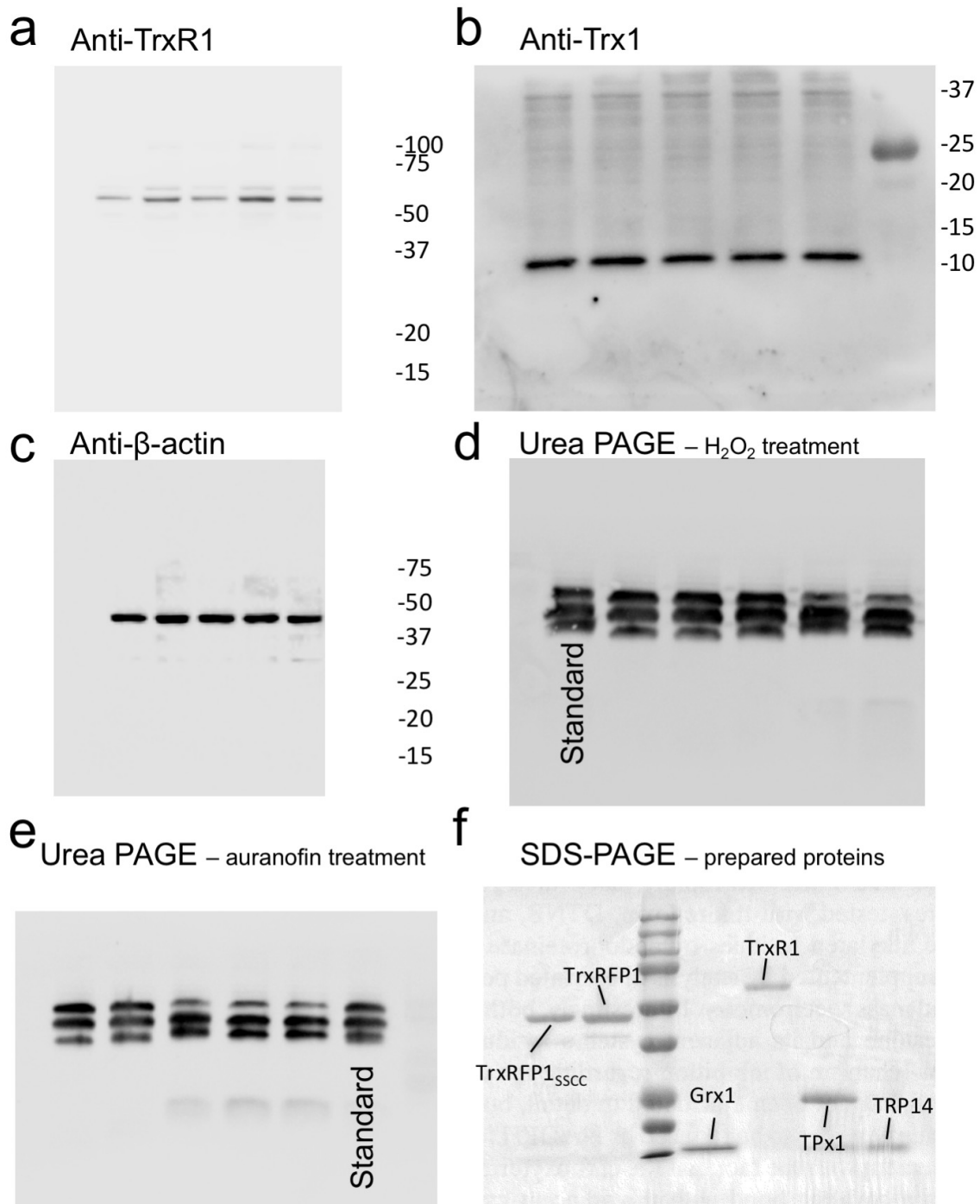
**Supplementary Figure 18.** Fluorescence responses of TrxRFP1 (red) or rxRFP1 (black) in the indicated cell lines to various concentrations of auranofin, confirming that TrxRFP1 is an effective probe for Trx redox changes under diverse conditions. Data are shown as mean and s.d. of three independent experiments.



**Supplementary Figure 19.** Time-lapse fluorescence images of HeLa cells expressing TrxRFP1 treated with 20 μM H<sub>2</sub>O<sub>2</sub> (a) or 5 μM auranofin (b), showing H<sub>2</sub>O<sub>2</sub>- and auranofin- induced Trx oxidation. H<sub>2</sub>O<sub>2</sub> and auranofin were added at 2 min and 10 min, respectively. In the top row are pseudocolored ratiometric images ( $F/F_0$ ), and in the bottom row are fluorescence images showing relative intensities. The experiments were repeated three times (Scale bar = 40 μm).



**Supplementary Figure 20.** Time-lapse responses of a genetically encoded pH indicator pHRFP in HEK 293T cells to serum stimulation (a) or EGF stimulation (b), showing no pH-induced fluorescence increase (Scale bar = 40  $\mu\text{m}$ ). In panels b and d, the intensities were normalized to the value at t = 0 min and shown as the mean and s.d. of randomly selected six cells from three independent replicates.



**Supplementary Figure 21.** Original immunoblots presented in the manuscript and an SDS-PAGE to show the purities of our prepared proteins.

## Supplementary Tables

**Supplementary Table 1. Oligonucleotides used in this study.**

Oligo name	Nucleotide sequence
Trx-F	GTTACTCGAGCATGGTTAAACAGATC
Trx-R	GCTAAGCTTAACCAGTTCGTTGATGG
0.1-R1	GCCACCACTGCCACCAACCAGTTCGTTGATGGT
0.1-R2	CCCTCCGCTCCCTCCACCGCCACTACCGCCGCCACCACTGCCACC
0.1-R3	CCCGCCACTTCCACCTCCCCCGTTCCTCCCCCTCCGCTCCCTCC
0.1-R4	TATAGCGCAACTAAGCTCGCCCCACTACCTCCCCGCCACTTCCACC
0.1-F	GGAGGTAGTGGGGGCGAGCTTAGTTGCGCTATA
2-R	AGAGCCGGAACCAGAAACCAGTTCGTTGAT
2-F	TCTGGTTCGGCTCTGAGCTTAGTTGCGCTATA
3-R	CATAGAGCCGGAACCAGAAGCCACACTGCAGCACCT
3-F	GCTTCTGGTTCGGCTCTATGGTTAAACAGATCGAATCT
TrxRFP3-R	GTCGATAAGCTTAAACCAGTTCGTTGATGGTCGC
4-R	ATGATGATGAGAACCCCAACCAGTTCGTTGAT
4-F	ATCAACGAACTGGTTGGGGGTTCTCATCATCAT
32S-R	TTTGCACGGACCGCTCCAGGTGCGAGA
32S-F	TCTGCGACCTGGAGCGGTCCGTGCAAA
35S-R	TTTGATCATTTTGTCTGGACCGCACCA
35S-F	TGGTGCGGTCCGAGCAAAATGATCAAA
32/35S-R	GATCATTTTGTCTGGACCGCTCCAGGT
32/35S-F	ACCTGGAGCGGTCCGAGCAAAATGATC
62S-R	TTCAGACGCAACGTCCTGGGAGTCGTC
69/73S-F	CAGGACGTTGCGTCTGAATCCGAAGTTAAATCCATGCCG
62/69C-R	TCAGACGCAACGTCCTGGCAGTCGTCAACG
62/69C-F	GACGTTGCGTCTGAATGCCGAAGTTAAATCC
0.2-F	ATCAACGAACTGGTTGGTGGATCCGGTGGCGGC
0.2-R	GCCGCCACCGGATCCACCAACCAGTTCGTTGAT
C397S-R	CTGAAGCTTAAGCCTGACTGGAGCACCTTTGGTCACG
C217Y-F	CCATCGTGGAACAGTACGAACGCGCCGAGGG
C217Y-R	CCCTCGGCGCGTTCGTAAGTTCACGATGG
TRND-F	GTTACTCGAGCATGAACGGCCCTGAAGAT
TRND-R	TAGCAAGCTTAGTAAGCGCAGCAGCCAGC
PRD-F	GTTACTCGAGCATGTCTTCAGGAAATGCT
PRD-R	TAGCAAGCTTACTACTTCTGCTTGAGAA
Grx-F	CACTCGAGAATGGCTCAAGAGTTTGTGA
Grx-R	CTAAGCTTAAGTCTGCAGAGCTCCAATCT
pBAD-F	ATGCCATAGCATTTTATCC
pBAD-R	GATTTAATCTGTATCAGG
CMV-F1	ATACTAAAGCTTGCCGCCACCATGGGAGGTTTCATCATCATCAT
CMV-TrxRFP1-R	CGTCTAGATTAAGCCTGACTGGAGCACCTTTGGTCACG
Nuc-R1	CTTCTTTTTTGGATCAGCCTGACTGGAGCACCTT
Nuc-R2	TCGTTTTTCTTCGGGTCTACCTTCTCTTCTTTTTTGGATC
Nuc-R3	CGATTCTAGATTACTTCTTCTTCTTCTTGGATCTACCTTTCGTTTTTCTTCGG
Mito-F	GACCCAAGCTTGCCGCCACCATGCTAT
Mito-TrxRFP-F	AATACGATTCTTCAAGCCAGCAA
Mito-TrxRFP-R	TTGCTGGCTTGAAGAATCGTATT

NES-F1	CTTGAACGTCTTACTCTTGGAGGTTTCATCATCAT
NES-F2	AAGAGTAAGACGTTCAAGAGGAGGAAGTTGAAGCATAAGCTTGAT
NES-R	ACTGTCTAGAAGCCTGACTGGAGCACCTTT
HyPer-F	ATCAAGCTTATGGAGATGGCAAGC
HyPer-R	CCGTCTAGATTAACCGCCTGTTT
HyPer-NES-F	CGTAGGATCCATGGAGATGGCAAGCCAG
HyPer-NES-R	CAGTCTAGAAACCGCCTGTTTTAAAAC
HyPer-Nuc-R1	CTTCTTTTTGGATCAACCGCCTGTTTTAAAAC

## Supplementary Videos

<b>Supplementary Video 1</b>	Responses of TrxRFP1 in HEK 293T to H <sub>2</sub> O <sub>2</sub> and DTT
<b>Supplementary Video 2</b>	Responses of TrxRFP1 in HEK 293T to auranofin
<b>Supplementary Video 3</b>	Responses of TrxRFP1 in HeLa to H <sub>2</sub> O <sub>2</sub>
<b>Supplementary Video 4</b>	Responses of TrxRFP1 in HeLa to auranofin
<b>Supplementary Video 5</b>	Simultaneous imaging of H <sub>2</sub> O <sub>2</sub> -induced Trx and glutathione dynamics
<b>Supplementary Video 6</b>	Simultaneous imaging of auranofin-induced Trx and glutathione dynamics
<b>Supplementary Video 7</b>	Simultaneous imaging of EGF-induced Trx and glutathione dynamics